JOURNAL OF
EMERGING INVESTIGATORS

Article

Assessing the efficacy of NOX enzyme inhibitors as potential treatments for ischemic stroke *in silico*

Samhita Vinay,* Keertana Yalamanchili,* Sowmya Vinay
Thomas Jefferson High School for Science & Technology, Alexandria, Virginia
*authors contributed equally

SUMMARY

Ischemic stroke occurs when blood flow to the brain is interrupted, causing brain damage. There is evidence that reactive oxygen species, ROS, are produced by the enzyme family NADPH oxidase (NOX) following ischemic stroke, which leads to further brain injury. This study investigated the effectiveness of different NOX inhibitors as treatments for ischemic stroke *in silico*. The ADMET (absorption, distribution, metabolism, excretion, and toxicity) profile of each NOX inhibitor was taken, in which four classifications, namely applicability domain, human intestinal absorption, blood-brain barrier, and human oral bioavailability, were observed. The profile was used to determine the properties of each inhibitor in order to examine the extent to which it will work as a drug candidate. Then, AutoDock Vina was used to model the docking of the inhibitors: VAS2870, GSK2795039, apocynin, and AEBSF to NOX2, an isoform of the NOX family. We hypothesized that VAS2870 would be the most effective inhibitor *in silico* due to its potency to NOX2, not present in the other inhibitors. The binding affinities of each of the inhibitors to NOX2 were recorded, and the value was used to calculate the K_i value of each inhibitor. VAS2870 and apocynin were the most potent NOX2 inhibitors, and all four inhibitors had favorable ADMET profiles. This study helps corroborate previous *in vivo* and *in vitro* studies in an *in silico* format, and can be used towards developing drugs to treat ischemic stroke.

INTRODUCTION

Ischemic stroke is a disease where a blocked blood vessel damages the brain by slowing down or interrupting blood flow (1). It accounts for approximately 88% of all strokes, and its onset can be influenced by several other diseases (2). It develops due to an improper supply of blood to the brain, which results in an inability for sufficient metabolism to occur, therefore restricting oxygen and glucose supply to the brain (3). The lack of sufficient oxygen and glucose supply compromises ion gradients, which allows cations to build up in the cells and further stimulates proteolytic activity causing neuronal apoptosis and the systematic degradation of the extracellular matrix (3). This process breaks the basal lamina, which results in leakage, undermining the integrity of the blood-brain barrier and causing an inflow of inflammatory cells into the brain, ultimately causing neuronal death (4). The blood-brain barrier is vital for controlling homeostasis in the central nervous system and protecting neural tissue from toxic substances (5). Therefore, its disruption can lead to inflammation of the brain, known as vasogenic edema, and a hemorrhage. Following ischemic stroke, reactive oxygen species (ROS) are produced, leading to further brain damage (6). Normally, oxygen-derived free radicals, often known as ROS, play roles in immunity and cell signaling; however, in excess, they lead to several diseases including ischemic stroke (7). Enzymes known as NADPH oxidases, which are in the NOX family, are attributed to producing ROS in human cells. Along with Rac as a binding partner, NOX2 is composed of isoforms and subunits, the former being NOX1-5, Duox1, and Duox2, and the latter being $p22^{phox}$, $p47^{phox}$, $p67^{phox}$, and $p40^{phox}$ (8). As a key element of the electron transport chain in cellular respiration, the ROS are produced by reducing electrons in oxygen. The family of enzymes was first found in the neutrophils and macrophages of the human immune system. Now, however, *in vivo* and *in vitro* studies suggest that NOX1, NOX2, NOX3, and NOX4 are expressed throughout the central nervous system, although their function with respect to the brain is unknown. Various studies have also confirmed that NOX enzymes, along with the ROS produced, play a role in brain injury progression following ischemic stroke (9).

In vivo and *in vitro* studies have determined several viable inhibitors of NOX2, which can be incorporated in ischemic stroke drug treatment. In this study, four inhibitors of the NOX2 isoform were selected including VAS2870, GSK2795039, AEBSF, and Apocynin, and their efficacy as potential ischemic stroke treatments was assessed. These four inhibitors were selected because they were the only inhibitors with 3D structures in the PubChem Database. NOX2 was the enzyme we focused on due to its high expression levels in endothelial cells in the brain (9), as well as the fact that its 3D model was the most accessible out of all the isoforms. VAS2870 is an artificial inhibitor that inhibits all NOX isoforms except NOX3 (10). Studies have demonstrated that VAS2870 leads to neuroprotective effects in mice that are not displayed in control groups (11). GSK2795039 is another artificially constructed inhibitor which competitively

inhibits NOX2 and reduces ROS production (12). In addition, AEBSF can block the binding of the subunits $p47^{phox}$ and $p67^{phox}$ as an irreversible inhibitor (11); however, it also is an inhibitor of serine proteases, which enzymatically break peptide bonds (13). Lastly, apocynin, is an antioxidant, and studies demonstrated that prior to ischemic stroke, the inhibitor showed neuroprotection and reduced blood-brain barrier disruption (11).

Here, we used ADMET (absorption, distribution, metabolism, excretion, and toxicity) to assess the biochemical properties of our four aforementioned inhibitors (14). ADMET is important when discovering new drugs because an accurate prediction of these properties can determine if the drug will work as intended (15). Although the ADMET properties are considered at the end of the drug testing process, they are now accounted for while eliminating potential docking molecules in order to improve efficiency and decrease associated costs. There are several classification systems that are used to assess drug molecules, namely applicability domain, human intestinal absorption, blood-brain barrier, and human oral bioavailability. The applicability domain considers whether the molecule is within the domain of the training set for six different properties: molecular weight, alogP, number of atoms, number of rings, H-bond acceptors, and H-bond donors (16). alogP is an atom-based method for predicting logP, which is the logarithm of the ratio of a solute among two solvents, also known as the partition coefficient (17). The human intestinal absorption classification determines how effectively orally administered drugs are absorbed from the intestine into the bloodstream (18). The blood-brain barrier classification shows how easily molecules can cross through the highly selective semipermeable barrier (19). The human oral bioavailability classification depicts how much of the drug reaches the target area (20). The ADMET properties for each molecule are represented with a predicted value and a predicted probability to display the drug's efficacy (19).

In addition to ADMET properties, we also will utilize molecular docking, which is a modeling technique that is used for discovering new drugs by determining how well one molecule can bind to another molecular structure (21). The orientation with which a molecule binds to a target can be used to assess its effectiveness (22). There are several types of docking, and the more commonly used types include protein-ligand docking and protein-protein docking (23). Protein-ligand docking can be used to determine how a ligand will bind to a protein and whether or not the ligand will act as an inhibitor or an activator (24). Protein-protein docking is an easier technique because the docking between the two proteins can be either flexible or rigid, meaning that precise measurement is not necessary (23). Molecular docking can be performed via various applications. AutoDock is one type of software that simulates an automated docking technique (25). The software contains AutoDock Vina, which is a program that performs protein-ligand docking by using an empirical scoring function and a conformation search based on global optimization (26).

We hypothesized that out of the four inhibitors: VAS2870, GSK2795039, AEBSF, and apocynin, VAS2870 would be the most effective inhibitor *in silico* because previous *in vivo* and *in vitro* studies revealed that it successfully inhibited NOX2, while the efficacy of the other inhibitors was not mentioned (10). The data from the study showed that VAS2870 and apocynin were the most potent NOX2 inhibitors and that all four inhibitors had favorable ADMET profiles. These results can be used for developing medication for ischemic stroke in the future.

RESULTS

The ADMET profiles of the four different inhibitors: apocynin, VAS2870, GSK2795039, and AEBSF were assessed using admetSAR (16). For each inhibitor, four different classifications were observed: the applicability domain, human intestinal absorption, blood-brain barrier, and human oral bioavailability. All four inhibitors are in the applicability domain, meaning that the admetSAR interface can use its training set to predict their properties. In terms of the human intestinal absorption classification, all four inhibitors have a "+" predicted value as well as predicted

Table 1. ADMET properties of different inhibitors.

Inhibitor	*Applicability Domain*	*Human Intestinal Absorption*	*Blood-Brain Barrier*	*Human Oral Bioavailability*
apocynin	In domain	+; 1.0000	+; 0.9483	+; 0.5857
VAS2870	In domain	+; 0.9820	+; 0.9785	+; 0.5286
GSK2795039	In domain	+; 0.9947	+; 0.9750	+; 0.6143
AEBSF	In domain	+; 0.9656	+; 0.9733	+; 0.8857

Note: The "+" or "-" represent whether the molecule does or does not display the particular property, respectively. The predicted probability is depicted by a number between 0 and 1, which shows the probability of the molecule acting as indicated by the previously mentioned predicted value (19). The "In domain" shows that the compound falls into the range established by 99% of the training set.

Table 2. Descriptive statistics of each inhibitor.

Binding Energy (kcal/mol)	Inhibitors			
	apocynin	VAS2870	GSK2795039	AEBSF
Mean	-7.2	-7.2	-6.4	-4.5
Median	-7.2	-7.2	-6.3	-4.4
S.D.	0.0	0.0	0.2	0.1
Number	5	5	5	5
SEM	0.0	0.0	0.1	0.1
K_i	$5.2*10^{-6}$	$5.2*10^{-6}$	$2.0*10^{-5}$	$5.0*10^{-4}$

Note: The values represent the binding energies in kcal/mol. The table includes means, medians, standard deviations, the number of data points used, the standard error of the mean, and inhibitor constants.

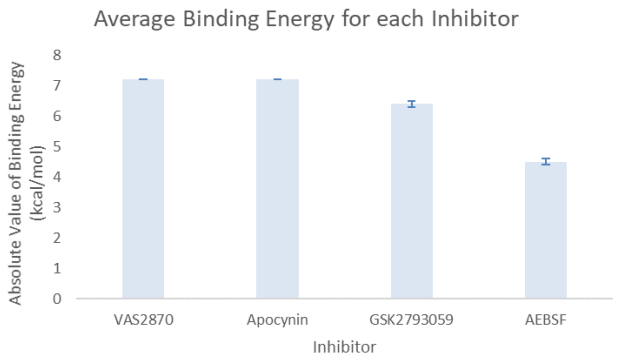

Figure 1. Average binding energy of each inhibitor. The data represents the absolute value of the average binding energies (in kcal/mol) +/- 1 standard error. For each average value, 5 trials were conducted.

probabilities greater than 0.95 (**Table 1**), meaning that they can probably be absorbed from the intestine into the bloodstream. Furthermore, all four inhibitors have a "+" predicted value and a predicted probability greater than 0.945 for the blood-brain barrier classification, meaning that they can probably pass through the membrane effectively (**Table 1**). Lastly, although all four inhibitors have a "+" predicted value (**Table 1**) for the human oral bioavailability classification, their predicted probabilities are low and lie between 0.55 and 0.65, except for AEBSF, which has a predicted probability of 0.8857. Although the human oral bioavailability probabilities of apocynin, VAS2870, and GSK2705039 are closer to 0.5 than to 1, overall, all four inhibitors have favorable ADMET profiles.

Blind docking analysis using AutoDock Vina was used to analyze the efficacy of the four NOX2 inhibitors as potential treatments for ischemic stroke. The average binding affinities of VAS2870 and apocynin were equal, at -7.2 kcal/mol, while that of GSK2795039 and AEBSF were -6.4 kcal/mol and -4.5 kcal/mol respectively (**Table 2**). The negative binding affinities of all the inhibitors suggest binding to NOX2 is stable. The K_i value for each inhibitor, which was calculated for each inhibitor, and the lower the value, the more potent the inhibitor (**Table 2**). The K_i value of $5.2 * 10^{-6}$ was the lowest, demonstrating that VAS2870 and apocynin are predicted to be the most potent inhibitors of NOX2. AEBSF was the least potent NOX2 inhibitor, as its K_i value of $5.0 * 10^{-4}$ was the greatest value. The range of the binding affinity of each inhibitor as displayed by standard deviation was relatively low, with all of them having values at or close to 0.0 (**Table 2**).

Next, we determined the absolute value binding energies of each inhibitor by calculating the average binding energy of five trials for each inhibitor and taking the absolute value of the result (**Figure 1**). There was little to no variation between the absolute values of the binding energies of each inhibitor (**Figure 1**). VAS2870 and apocynin had the same average absolute value binding energy, with standard errors of 0. Both GSK2795039 and AEBSF had slightly larger standard errors of 0.1. The standard errors of GSK2795039 and AEBSF do not overlap (**Figure 1**). Those of VAS2870 and apocynin only overlap because the data was the same with no variation.

Lastly, we used a Kruskal-Wallis test to analyze whether the differences in the binding affinities of the inhibitors were statistically significant or not, as the data was not normally distributed. According to the test, there was a statistically significant difference in the binding energies of the different inhibitors, $\chi^2(3, N = 20) = 18.411$, p-value < 0.001. Results from the Dunn-Bonferroni post-hoc tests revealed that VAS2870 and apocynin were significantly different from AEBSF (p-value 0.001, adjusted to 0.006), but not GSK2795039 (0.015, adjusted to 0.090) in terms of binding energies (kcal/mol). When VAS2870 was compared to apocynin, the p-value and Bonferroni-corrected p-value were both 1.000, since the averages were the same. The pairwise comparison between GSK2795039 and AEBSF resulted in a p-value of 0.391 and a Bonferroni-corrected p-value of 1.000.

DISCUSSION

The purpose of this study was to investigate the effectiveness of four NOX2 inhibitors *in silico* so that they may eventually be candidates for drugs against ischemic stroke. This was accomplished through downloading models of NOX2 and each of the inhibitors and simulating how the inhibitors dock to NOX2 using AutoDock Vina. ADMET profiles of all the inhibitors were also assessed through taking into account the applicability domain, human intestinal absorption, blood-brain barrier, and human oral bioavailability. Following this, the Ki values for each of the inhibitors were calculated to assess the potency of each of the inhibitors. Overall, the data supported our hypothesis that VAS2870 would be the most potent inhibitor of NOX2, but it did not account for the fact that apocynin was equally as potent, and that there was no significant difference between the binding energies of VAS2870/apocynin and GSK2795039. Nevertheless, all the inhibitors were predicted to inhibit the NOX2 enzymes, and they all had favorable ADMET profiles.

In silico studies confer many advantages in early-stage drug development compared to *in vivo* and *in vitro* studies, such as speed and the ability to predict a molecule's properties before synthesis (27). Furthermore, they can be more representative of human body systems than animal models in terms of identifying side effects and determining how effective the drugs are (28). However, there may have been possible errors in the docking methodology. For example, the protein flexibility and molecule conformation may not have been accounted for properly by the AutoDock Vina program, resulting in inaccurate data. Furthermore, *in silico* docking softwares typically use an algorithm based on human properties, whereas *in vivo* and *in vitro* use a variety of other species. As a result, *in silico* findings cannot be considered as a complete replacement for *in vivo* and *in vitro* findings. Instead, they are a way to model and predict what

the docking might look like if it was conducted *in vivo* or *in vitro*.

To our knowledge, this is the first in silico study investigating the NOX2 enzymatic pathway as a possible treatment for ischemic stroke. *In vivo* and *in vitro* studies have illustrated that inhibiting the NOX2 enzyme led to neuroprotective effects following ischemic stroke by reducing ROS production (10-12). Although this study could not assess the behavior of animal models after this treatment, it demonstrates that these pharmacologically important inhibitors have the potential to be incorporated in drugs used to treat brain injury following ischemic stroke. The study also supports the findings of the *in vivo* and *in vitro* studies, as all of the inhibitors modeled were determined to be potent.

Further research on the docking of the NOX2 inhibitors *in vivo* and *in vitro* would be helpful to corroborate the results of this study. The additional research would more accurately consider protein flexibility and molecule conformation when determining the binding affinities of the inhibitors. Other compounds could also be tested and verified as inhibitors in future studies. For example, recombinant tissue plasminogen activator (rtPA), a compound for treating ischemic stroke, has a favorable ADMET profile, with a predicted probability of 0.902 for human intestinal absorption, 0.984 for passing through the blood-brain Barrier, and 0.723 for human oral bioavailability (29). Although rtPA has a higher predicted probability for passing through the blood-brain Barrier than the four inhibitors we observed (VAS2870, apocynin, GSK2795039, and AEBSF), the predicted probability of rtPA for human intestinal absorption is lower than the probabilities predicted for the four inhibitors we observed. In terms of human oral bioavailability, rtPA has a higher predicted probability than VAS2870, apocynin, and GSK295039, but a lower predicted probability than AEBSF. Moreover, it would also show how the docking occurs in different species. Although AutoDock Vina was used due to its user-friendliness, future studies could use additional platforms for molecular docking, such as SwissDock and UCSF Dock Blaster, to test not only the efficacy of AutoDock Vina, but also the consistency of binding scores and docking visualization.

METHODS

ADMET

ADMET Profiling: A unique SMILES (Simplified Molecular Input Line Entry System) notation, representing different molecules, was found for each inhibitor by entering the name of the inhibitor in the search tool in the PubChem website. The SMILES notation for each inhibitor was entered in the search box of the "Predict" tool of the admetSAR web tool. Several of the classifications, particularly the applicability domain, human intestinal absorption, blood-brain barrier, and human oral bioavailability, were taken into account when determining whether the ADMET profile of the inhibitor was favorable or not.

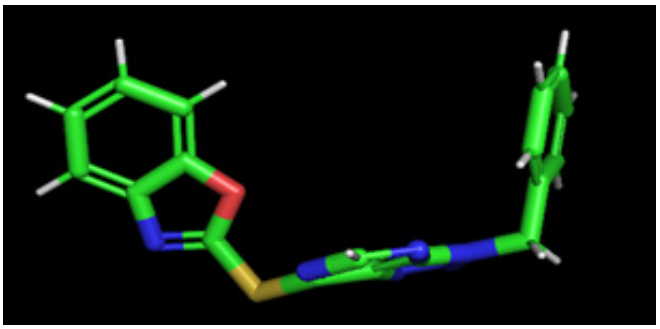

Figure 2. SDF file of VAS2870 displayed in PyMOL. The image shows the 3D structure of the inhibitor. The green parts of the structure represent the carbons, the red signifies oxygen, the blue represents nitrogen, the yellow signifies sulfur, and the gray extensions represent hydrogens.

Downloading & File Modification

Downloading: AutoDock Vina, AutoDock Tools, and PyMOL were downloaded onto the laptop from their respective websites online (30-32). The protein molecule 3A1F (the crystal structure of NOX2) was downloaded from the database RCSB PDB as a PDB file into a folder in the desktop with the licensing of AutoDock Vina (33). The 3D conformation of the inhibitor molecules: VAS2870, GSK2795039, apocynin, and AEBSF were downloaded from the PubChem database as SDF files into the same folder (**Figure 2**; 34-37).

SDF to PDB Conversion: The SDF file of the 3D structure of each inhibitor was uploaded into PyMOL, and then saved as a PDB file to the same folder that the SDF files were initially.
Protein Modification: The PDB file of 3A1F was opened as a text document, and all the lines with "HETATOM" were deleted, as the structure came with the nickel molecule (labeled with "HETATOM") already bound to the protein.
PDB to PDBQT Conversion: AutoDock Tools was opened, and then the PDB file of each of the inhibitors was uploaded and saved as a PDBQT file.

Several modifications were made for the NOX2 PDB conversion including removing waters, since waters are not included in the binding process, and adding hydrogens, because it adds to the stability of the protein (38). Following the chemical modification of the protein, a grid was set up so that the whole protein could be screened for potential binding sites. For this to occur, the number of points in the x, y, and z-dimensions were set to 126. The spacing was set to 0.375 angstroms, and the x, y, and z-centers were set to 15.597, -13.324, and 10.201 respectively. Then, a text file of the grid information was saved in the same folder, along with the protein in PDBQT format.

Configuration File Creation: A configuration file, conf.txt, was created in order to specify the receptor and the ligand molecule to be used for the docking. In the file, the receptor was set to the protein file name, and the ligand was set to the inhibitor file name. The center-x, center-y, and center-z

```
center_x= 15.597

center_y= -13.324

center_z=  10.201
```

Figure 3. Coordinates of the center of NOX2 in the configuration file. The variables center_x, center_y, and center_z represent the x, y, and z coordinates of the grid, respectively. These coordinates were used to align each of the inhibitors to the protein.

were set according to the centers used in the grid dimensions (**Figure 3**), and the sizes of x, y, and z were set to 66, 56, and 54 respectively. The output was set to another PDBQT file named vina_outSO.pdbqt, the log was set to logSO.txt, and the exhaustiveness was set to 8. The ligand of the file was altered each time a new inhibitor was used for docking.

Molecular Docking

Docking: A command prompt was opened, and the desktop folder with all the necessary components was accessed by typing in "cd Desktop" and then "cd Vina". In order to find the binding affinity of the inhibitors with NOX2, "vina.exe" --config conf.txt was typed. This command ran blind docking analysis, assessing all the potential locations in which the inhibitor can bind to NOX2. After the analysis was complete, a table of binding affinities, distance from RMSD lower bound, and distance from RMSD upper bound appeared, detailing the results of each potential binding site for the docking analysis. This process was repeated four times for each inhibitor and for other inhibitors by altering conf.txt and running the blind docking for each inhibitor.

3D Visualization: the output ligand and NOX2 were uploaded into PyMOL, a visualization software. In order to show the interactions between the protein and the ligand, we visualized contacts of chains between 3.0Å, 3.5Å, and 4.0Å, which were shown in a dotted line.

Analysis

K_i value calculation: the average binding affinity was taken for each inhibitor, and then converted to a K_i value, also known as the inhibition constant. The equation, $K_i = e^{(deltaG/(RT))}$, was used for the conversion, where the binding affinity was substituted for the delta G value, R was the gas constant of 1.987 cal/molK, and T was the temperature: 298 K.

Statistical analysis: The standard errors were calculated by dividing the standard deviation by the square root of the number of trials, which was 5. Afterwards, a Kruskal-Wallis test was used to determine the statistical significance of the difference in the binding affinity of each inhibitor. This non-parametric test was used, since a normal distribution is not assumed, and as there were four levels of the independent variable that needed to be analyzed. Following this, a Dunn-Bonferroni post-hoc test was performed to see whether there were statistically significant differences between the groups. A Bonferroni Correction was applied for each significance value to account for errors due to multiple comparisons.

Received: May 20, 2020
Accepted: August 31, 2020
Published: September 18, 2020

REFERENCES

1. "Stroke." *Mayo Clinic*, Mayo Foundation for Medical Education and Research, 24 Apr. 2020, www.mayoclinic.org/diseases-conditions/stroke/symptoms-causes/syc-20350113.
2. "The Internet Stroke Center." *The Internet Stroke Center. An Independent Web Resource for Information about Stroke Care and Research.*, www.strokecenter.org/patients/about-stroke/ischemic-stroke/.
3. Bhattacharya, Pallab, *et al.* "Neuroprotection by μ-Calpain and Matrix Metalloproteinases Inhibition by Piroxicam in Cerebral Ischemia: an in Silico Study." *Medicinal Chemistry Research*, vol. 22, no. 11, 2013, pp. 5112–5119., doi:10.1007/s00044-013-0514-7.
4. Bramlett, Helen M., and W. Dalton Dietrich. "Pathophysiology of Cerebral Ischemia and Brain Trauma: Similarities and Differences." *Journal of Cerebral Blood Flow & Metabolism*, vol. 24, no. 2, 2004, pp. 133–150., doi:10.1097/01.wcb.0000111614.19196.04.
5. Abdullahi, Wazir, *et al.* "Blood-Brain Barrier Dysfunction in Ischemic Stroke: Targeting Tight Junctions and Transporters for Vascular Protection." *American Journal of Physiology-Cell Physiology*, vol. 315, no. 3, 2018, doi:10.1152/ajpcell.00095.2018.
6. Rodrigo, Ramon, *et al.* "Oxidative Stress and Pathophysiology of Ischemic Stroke: Novel Therapeutic Opportunities." *CNS & Neurological Disorders - Drug Targets*, vol. 12, no. 5, 2013, pp. 698–714., doi:10.2174/18715272311312050015.
7. Panday, Arvind, *et al.* "NADPH Oxidases: an Overview from Structure to Innate Immunity-Associated Pathologies." *Cellular & Molecular Immunology*, vol. 12, no. 1, 2014, pp. 5–23., doi:10.1038/cmi.2014.89.
8. Lassègue, Bernard, *et al.* "Biochemistry, Physiology, and Pathophysiology of NADPH Oxidases in the Cardiovascular System." *Circulation Research*, vol. 110, no. 10, 2012, pp. 1364–1390., doi:10.1161/circresaha.111.243972.
9. Zhang, Li, *et al.* "NADPH Oxidase: A Potential Target for Treatment of Stroke." *Oxidative Medicine and Cellular Longevity*, vol. 2016, 2016, pp. 1–9., doi:10.1155/2016/5026984.
10. Augsburger, Fiona, *et al.* "Pharmacological

Characterization of the Seven Human NOX Isoforms and Their Inhibitors." *Redox Biology*, vol. 26, 2019, 101272., doi:10.1016/j.redox.2019.101272.
11. Kim, Jong Youl, *et al.* "NOX Inhibitors - A Promising Avenue for Ischemic Stroke." *Experimental Neurobiology*, vol. 26, no. 4, 2017, pp. 195–205., doi:10.5607/en.2017.26.4.195.
12. Hirano, Kazufumi, *et al*. "Discovery of GSK2795039, a Novel Small Molecule NADPH Oxidase 2 Inhibitor." *Antioxidants & Redox Signaling*, vol. 23, no. 5, 2015, pp. 358–374., doi:10.1089/ars.2014.6202.
13. Poddar, Nitesh Kumar, *et al*. "Role of Serine Proteases and Inhibitors in Cancer." *Proteases in Physiology and Pathology*, 2017, pp. 257–287., doi:10.1007/978-981-10-2513-6_12.
14. Guan, Longfei, *et al*. "ADMET-Score – a Comprehensive Scoring Function for Evaluation of Chemical Drug-Likeness." *MedChemComm*, vol. 10, no. 1, 2019, pp. 148–157., doi:10.1039/c8md00472b.
15. G. P. S. Raghava's Group. *Computational Tools for ADMET*, crdd.osdd.net/admet.php.
16. "Applicability Domain." *AD | AdmetSAR*, lmmd.ecust.edu.cn/admetsar2/about/ad.
17. Ghose, Arup K., *et al*. "Prediction of Hydrophobic (Lipophilic) Properties of Small Organic Molecules Using Fragmental Methods: An Analysis of ALOGP and CLOGP Methods." *The Journal of Physical Chemistry A*, vol. 102, no. 21, 1998, pp. 3762–3772., doi:10.1021/jp980230o.
18. Isle Interactive Ltd. "Human Intestinal Absorption." *Isle Spark*, www.asteris-app.com/technical-info/adme-properties/humanintestinalabsorption.htm.
19. "blood-brain Barrier." *DrugBank Developer Hub*, ev.drugbankplus.com/guides/terms/blood-brain-barrier.
20. Kim, Marlene T., *et al*. "Critical Evaluation of Human Oral Bioavailability for Pharmaceutical Drugs by Using Various Cheminformatics Approaches." *Pharmaceutical Research*, vol. 31, no. 4, 2013, pp. 1002–1014., doi:10.1007/s11095-013-1222-1.
21. Berry, Michael, *et al.* "Practical Considerations in Virtual Screening and Molecular Docking." *Emerging Trends in Computational Biology, Bioinformatics, and Systems Biology*, 2015, pp. 487–502., doi:10.1016/b978-0-12-802508-6.00027-2.
22. Hakes, L., *et al*. "Specificity in Protein Interactions and Its Relationship with Sequence Diversity and Coevolution." *Proceedings of the National Academy of Sciences*, vol. 104, no. 19, 2007, pp. 7999–8004., doi:10.1073/pnas.0609962104.
23. Hernandez-Santoyo, Alejandra, *et al*. "Protein-Protein and Protein-Ligand Docking." *Protein Engineering - Technology and Application*, 2013, doi:10.5772/56376.
24. Smith, Richard D., *et al*. "Biophysical Limits of Protein–Ligand Binding." *Journal of Chemical Information and Modeling*, vol. 52, no. 8, 2012, pp. 2098–2106., doi:10.1021/ci200612f.
25. "AutoDock." *AutoDock - an Overview | ScienceDirect Topics*, www.sciencedirect.com/topics/biochemistry-genetics-and-molecular-biology/autodock.
26. Trott, Oleg, and Arthur J. Olson. "AutoDock Vina: Improving the Speed and Accuracy of Docking with a New Scoring Function, Efficient Optimization, and Multithreading." *Journal of Computational Chemistry*, 2009, doi:10.1002/jcc.21334.
27. Amberg, Alexander. "In Silico Methods." *Drug Discovery and Evaluation: Safety and Pharmacokinetic Assays*, 2013, pp. 1273–1296., doi:10.1007/978-3-642-25240-2_55.
28. Coleman, Robert A. "Human Tissue in the Evaluation of Safety and Efficacy of New Medicines: A Viable Alternative to Animal Models?" *ISRN Pharmaceutics*, vol. 2011, 2011, pp. 1–8., doi:10.5402/2011/806789.
29. Dong, Jie. "Home-ADMElab: ADMET Prediction: ADMET Predictor: QSAR: ADMET Database." *Home-ADMElab: ADMET Prediction|ADMET Predictor|QSAR|ADMET Database*, admet.scbdd.com/.
30. "Download:" *AutoDock Vina - Molecular Docking and Virtual Screening Program*, vina.scripps.edu/download.html.
31. "Downloads." *MGLTools*, mgltools.scripps.edu/downloads.
32. "PyMOL Is a User-Sponsored Molecular Visualization System on an Open-Source Foundation, Maintained and Distributed by Schrödinger. We Are Happy to IntroducePyMOL 2.4!" *PyMOL*, pymol.org/2/#download.
33. Bank, RCSB Protein Data. "3A1F: The Crystal Structure of NADPH Binding Domain of gp91(Phox)." *RCSB PDB*, www.rcsb.org/structure/3a1f.
34. "2-(3-Benzyltriazolo[4,5-d]Pyrimidin-7-Yl)Sulfanyl-1,3-Benzoxazole." *National Center for Biotechnology Information. PubChem Compound Database*, U.S. National Library of Medicine, pubchem.ncbi.nlm.nih.gov/compound/vas2870.
35. "1-Methyl-N-[3-(1-Methyl-2,3-Dihydroindol-6-Yl)-1-Propan-2-Ylpyrrolo[2,3-b]Pyridin-4-Yl]Pyrazole-3-Sulfonamide." *National Center for Biotechnology Information. PubChem Compound Database*, U.S. National Library of Medicine, pubchem.ncbi.nlm.nih.gov/compound/71090129.
36. "Acetovanillone." *National Center for Biotechnology Information. PubChem Compound Database*, U.S. National Library of Medicine, pubchem.ncbi.nlm.nih.gov/compound/2214.
37. "4-(2-Aminoethyl)Benzenesulfonyl Fluoride." *National Center for Biotechnology Information. PubChem Compound Database*, U.S. National Library of Medicine, pubchem.ncbi.nlm.nih.gov/compound/1701.
38. "How to Perform Blind Docking Using AutoDock Vina?" *Bioinformatics Review*, 1 May 2019, bioinformaticsreview.com/20190501/how-to-perform-blind-docking-using-autodock-vina/.